Biogeosciences Discuss., https://doi.org/10.5194/bg-2017-521
Manuscript under review for journal Biogeosciences
Discussion started: 8 January 2018


Biogeosciences Discussions Open Access EGU

# $CO_2$ flux over young and snow-covered Arctic sea ice in winter and spring

Daiki Nomura[1, 2, 3*], Mats A. Granskog[4], Agneta Fransson[4], Melissa Chierici[5, 6], Anna Silyakova[7], Kay I. Ohshima[1, 3], Lana Cohen[4], Bruno Delille[8], Stephen R. Hudson[4], and Gerhard S. Dieckmann[9]

1 Institute of Low Temperature Science, Hokkaido University, Kita–19, Nishi–8, Kita–ku, Sapporo, Hokkaido 060–0819, Japan.

2 Faculty of Fisheries Sciences, Hokkaido University, 3–1–1, Minato–cho, Hakodate, Hokkaido 041–8611, Japan.

3 Arctic Research Center, Hokkaido University, Kita–21, Nishi–11, Kita–ku, Sapporo, Hokkaido 001–0021, Japan.

4 Norwegian Polar Institute, Fram Centre, NO–9296 Tromsø, Norway.

5 Institute of Marine Research, NO–9294, Tromsø, Norway.

6 FRAM-High North Research Centre for Climate and the Environment, Tromsø, Norway.

7 CAGE, Centre for Arctic Gas Hydrate, Environment and Climate, Tromsø, Norway.

8 Unité d'Océanographie Chimique, Université de Liège, Liège, Belgium.

9 Alfred Wegener Institute for Polar and Marine Research, Bremerhaven, Germany.

Biogeosciences Discuss., https://doi.org/10.5194/bg-2017-521
Manuscript under review for journal Biogeosciences
Discussion started: 8 January 2018


31 ＊Corresponding author: Daiki Nomura, e-mail: daiki.nomura@fish.hokudai.ac.jp,
32 Faculty of Fisheries Sciences, Hokkaido University, 3–1–1, Minato–cho, Hakodate,
33 Hokkaido 041–8611, Japan.
34
35
36

Biogeosciences Discuss., https://doi.org/10.5194/bg-2017-521
Manuscript under review for journal Biogeosciences
Discussion started: 8 January 2018


**Abstract**

We show that young, snow-covered ice has a potential for sea-ice-to-air $CO_2$ release during winter and spring in the Arctic Ocean north of Svalbard. Young thin sea ice was characterized by high salinities and thus porosity, while the surface of thicker sea ice was relatively warm (>–7.5°C), due to a thick insulating snow cover, even though air temperatures were as low as –40°C. During these conditions, brine volume fractions of sea ice were high, providing potentially favorable conditions for gas exchange between sea ice and overlying air even in mid-winter. Although the potential $CO_2$ flux through the sea ice decreased due to the presence of the snow, the snow surface still is a $CO_2$ source to the atmosphere for low snow density and thin snow conditions. Especially young ice formed in leads, without snow cover, is important for the $CO_2$ flux from the ice pack as the fluxes are an order of magnitude higher than for snow-covered older ice.

## 1 Introduction

Arctic sea ice is changing dramatically, with rapid declines in summer sea ice extent and a shift towards younger and thinner first-year ice rather than thick multi-year ice (e.g., Stroeve et al., 2012; Meier et al., 2014; Lindsay and Schweiger, 2015). Although the effects of sea ice formation and melting on biogeochemical cycles in the ocean have previously been discussed (e.g., Vancoppenolle et al., 2013), the effects of sea ice freezing and melting on the carbon dioxide ($CO_2$) exchange with the atmosphere are still large unknowns (Parmentier et al., 2013). Recent $CO_2$ flux measurements on sea ice indicate that sea ice is an active component in gas exchange between ocean and atmosphere (Nomura et al., 2013; Geilfus et al., 2013; 2014; Delille et al., 2014; Brown et al., 2015; Kotovitch et al., 2016). However, due to the difficulty in acquiring observations during winter, there is a definite lack of information on conditions during wintertime.



68 The sea ice $CO_2$ fluxes depend on (a) the difference in the partial pressure of $CO_2$
69 ($pCO_2$) between the sea ice surface and air, (b) ice surface condition including the snow
70 deposited on ice, and (c) wind-driven pressure pumping through the snow. For (a), it is
71 known that the air–sea ice $CO_2$ flux is driven by the differences in $pCO_2$ between the
72 sea ice surface and atmosphere (e.g. Delille et al., 2014; Geilfus et al., 2014). The brine
73 $pCO_2$ changes due to processes within the sea ice, such as thermodynamic process (e.g.,
74 Delille et al., 2014), biological activity (e.g., Delille et al., 2007; Fransson et al., 2013;
75 Rysgaard et al., 2013), and calcium carbonate ($CaCO_3$; ikaite) formation and dissolution
76 (e.g., Papadimitriou et al., 2012). When the $pCO_2$ in the brine is higher than that of the
77 air $pCO_2$, brine has the potential to release $CO_2$ to the atmosphere. For (b), the air–sea
78 ice $CO_2$ flux is strongly dependent on the sea ice surface conditions (Nomura et al.,
79 2010a, 2013; Geilfus et al., 2013; 2014; Barber et al., 2014; Brown et al., 2015;
80 Fransson et al., 2015). Nomura et al. (2013) proposed that snow conditions (e.g., water
81 equivalent) are important factors affecting gas exchange processes on sea ice. For (c), it
82 is thought that for snow cover, the $CO_2$ flux is affected by wind pumping (Takagi et al.,
83 2005) in which the magnitude of $CO_2$ flux through snow or overlying soil (e.g., Takagi
84 et al., 2005) increases due to wind pumping and can increase the transport with
85 molecular diffusion by up to 40% (Bowling and Massman, 2011). These results were
86 mainly found over land-based snow (soil and forest), and thus these processes are not
87 well understood over sea ice (Papakyriakou and Miller, 2011).
88
89 In addition to the processes described above, the $CO_2$ flux over sea ice may also be
90 influenced by the temperature difference between the ice surface and the atmosphere.
91 This has been shown in previous studies in dry snowpacks over land surfaces. These
92 studies show that there is an unstable air density gradient due to heating at the bottom
93 producing a strong temperature difference between bottom and top of snow (e.g.,
94 Powers et al., 1985; Severinghaus et al., 2010). This produces air flow within the
95 snowpack, which is a potentially significant contributor to mixing and transport of gas
96 and heat within the snowpack. We expect that this process would also occur in snow
97 over sea ice, especially during the wintertime when air temperatures are coldest and the
98 temperature difference between sea ice surface (snow bottom) and atmosphere is largest
99 (e.g., Massom et al., 2001). Generally, the sea ice surface under thick snow cover is

warm due to the heat conduction from the bottom of sea ice and the insulation effect of the snow cover, and a strong temperature difference between sea ice surface and atmosphere is observed (e.g., Massom et al., 2001). Such a temperature difference would produce an unstable air density gradient and upward transport of air containing $CO_2$ degassed at the sea-ice surface, thereby enhancing $CO_2$ exchange between sea ice and atmosphere.

The air–sea ice $CO_2$ flux was examined using flux chambers on Arctic pack ice north of Svalbard from mid-winter to spring (January to May 2015) during the Norwegian young sea ICE (N-ICE2015) campaign to understand the air–sea ice $CO_2$ flux during cold season, and effects of snow-cover on the air–sea ice $CO_2$ flux.

## 2 Materials and Methods

### 2.1 Study site

This study was performed during N-ICE2015 campaign with R/V Lance in the pack ice north of Svalbard from January to June 2015 (Granskog et al., 2016). Air–sea ice $CO_2$ flux measurements were carried out from January to May 2015 during the drift of Floes 1, 2, and 3 of the N-ICE2015 campaign (Figures 1 and 2, Table 1). The ice pack was a mixture of first-year ice and second-year ice (Granskog et al., 2017) both with a thick snow cover (Merkouriadi et al., 2017). In the N-ICE2015 study region modal ice thickness was about 1.3–1.5 m and modal snow thickness was almost 0.5 m (Rösel et al., 2016a and b). Formation of leads and their rapid refreezing provided us the opportunity to examine air–sea ice $CO_2$ fluxes over thin sea ice, occasionally covered with frost flowers (Figure 2 and Table 1). Air temperature and wind speed were measured at a 10 m weather mast on the ice floe installed about 400 m away from R/V Lance (Cohen et al., 2017).

Biogeosciences Discuss., https://doi.org/10.5194/bg-2017-521
Manuscript under review for journal Biogeosciences
Discussion started: 8 January 2018




132 **2.2 $CO_2$ flux measurements**

133

134 The air–sea ice $CO_2$ flux was measured with LI-COR 8100-104 chambers connected to
135 the LI-8100A soil $CO_2$ flux system (LI-COR Inc., USA) (Figure 2). This enclosed
136 chamber method has been widely applied over snow and sea ice (e.g., Schindlbacher et
137 al., 2007, Geilfus et al., 2015). Two chambers were connected in a closed loop to the
138 infrared gas analyzer (LI-8100A, LI-COR Inc., USA) to measure $CO_2$ concentration
139 through the multiplexer (LI-8150, LI-COR Inc., USA) with an air pump rate at 3 L $min^{-1}$
140 . Electricity was supplied by a car battery (8012-254, Optima Batteries Inc., USA).
141 Four $CO_2$ standards (324–406 ppmv) traceable to the WMO scale (Inoue and Ishii,
142 2005) were prepared to calibrate the $CO_2$ gas analyzer prior to the observations. $CO_2$
143 flux was measured from morning or afternoon during low-wind conditions (Table 2), to
144 minimize the effect of wind on the flux.

145

146 One chamber was installed over undisturbed snow or frost flowers over the ice surface.
147 The chamber collar was inserted 5 cm into the snow and 1 cm into ice at frost flowers
148 site to avoid air leaks between inside and outside of chamber. The second chamber was
149 installed after removing the snow or frost flowers. Flux measurements was begun
150 immediately in order to minimize the changes of the ice surface condition, and the data
151 of first $CO_2$ flux measurement was used. In order to evaluate the effect of removing
152 snow on sea ice surface temperature, ice surface temperature was monitored during $CO_2$
153 flux measurements at station FI6. To measure the sea ice surface temperature,
154 temperature sensor (RTR 52, T & D Corp., Japan) was installed in the top of the ice (1
155 cm) surface after snow removal. During first $CO_2$ flux measurements (about 30
156 minutes), ice surface temperature was stable at –5.8°C, suggesting that the effect of
157 removing snow on the variation of sea ice surface temperature was negligible. The
158 chamber was closed for 20 minutes in a sequence. The 20-minute time period was used
159 because $CO_2$ fluxes over sea ice are much smaller than over land. The $CO_2$
160 concentrations within the chamber were monitored to ensure that they changed linearly
161 throughout the measurement period. The $CO_2$ flux (mmol C $m^{-2}$ $day^{-1}$) (positive value
162 indicates $CO_2$ being released from air to ice surface) was calculated based on the
163 changes of the $CO_2$ concentration within the headspace of the chamber with LI-COR

software (Model: LI8100PC Client v.3.0.1.). The mean coefficient of variation for $CO_2$ flux measurements was less than 3.0% for $CO_2$ flux values larger than ±0.1 mmol C $m^{-2}$ $day^{-1}$. For $CO_2$ flux values smaller than ±0.1 mmol C $m^{-2}$ $day^{-1}$, the mean coefficient of variation for $CO_2$ flux measurements was higher than 3.0%, suggesting that the detection limit of this system is about 0.1 mmol C $m^{-2}$ $day^{-1}$.

In this paper, we express the $CO_2$ flux measured over the snow and frost flower as $F_{snow}$ and $F_{ff}$, respectively, and the flux measured directly over the sea ice surface either on snow-free ice or after removal of snow and frost flower as $F_{ice}$. $F_{snow}$ and $F_{ff}$ are the natural flux (snow and frost flowers are part of the natural system), and $F_{ice}$ is the potential flux in cases when snow or frost flowers are removed. While removal of snow and frost flowers is an artificial situation, comparisons between $F_{ice}$ and $F_{snow}$ or $F_{ff}$ provide information about the effect of snow on the $CO_2$ flux. Therefore, in this study, we discuss both situations for $CO_2$ flux.

### 2.3 Sampling of snow, frost flowers, brine, and sea ice

For salinity measurements, snow was sampled, while frost flowers and surface of sea ice after removing snow were sampled in bulk using a plastic shovel and taken into plastic bag and placed in an insulated box for transport to the ship-lab for further processing. These samples were melted slowly (2–3 days) in dark at +4°C. Temperature of the snow and frost flowers were measured using a needle-type temperature sensor (Testo 110 NTC, Brandt Instruments, Inc., USA). Accuracy of this sensor was ±0.2°C. Snow density was obtained by a fixed volume sampler (Climate Engineering, Japan) and weight measurement. The depth of the snow pack and frost flowers was also recorded using a ruler.

Brine was collected for determination of salinity, dissolved inorganic carbon (DIC) and total alkalinity (TA) for stations FI3–6 using the sackhole (Gleitz et al., 1995). First, sackholes were drilled using an ice corer (Mark II coring system, Kovacs Enterprises, Inc., USA) for 30 cm deep. The sackholes were covered with a lid made by 5 cm-thick

urethane to reduce heat and gas transfer between brine and atmosphere. When the brine accumulated at the bottom of the sackholes (approximately 15 minutes), the brine was collected with a plastic syringe (AS ONE Corporation, Japan) and kept in 500 mL unbreakable plastic bottles (I-Boy, AS ONE Corporation, Japan) due to cold and harsh conditions, as well as challenging transportation to the sampling sites. The brine bottle without head-space was immediately put into an insulated box to prevent it from freezing. Immediately after return to the ship, the brine samples were transferred to 250 mL borosilicate bottles (DURAN Group GmbH, Germany) for DIC and TA measurements using tubing to prevent contact with air. The samples were preserved with saturated mercuric chloride ($HgCl_2$, 60 µL for a 250 mL sample) and stored in dark at +10°C until analyses at the Institute of Marine Research, Norway.

Sea ice was collected by same ice corer as described for brine collection at the same location as snow and frost flowers were collected. Ice temperature was measured by same sensor as described for snow on ice. Temperature sensor was inserted in holes drilled into the core. Then, the core was cut with a stainless steel saw into 10 cm sections for salinity and the ice sections placed into plastic bags. Sections were then kept at +4°C and melted in the dark.

### 2.4 Sample analysis

Salinities for melted-snow, -frost flowers, -sea ice, and brine were measured with a conductivity sensor (Cond 315i, WTW GmbH, Germany). For calibration of salinity measurement, a salinometer Guildline PORTASAL Model 8410A, standardized by International Association for the Physical Sciences of the Oceans (IAPSO) standard seawater (Ocean Scientific International Ltd, UK) were used. Accuracy of this sensor was ±0.003.

Analytical methods for DIC and TA determination are fully described in Dickson et al. (2007). DIC in brine was determined using gas extraction of acidified sample followed by coulometric titration and photometric detection using a Versatile Instrument for the

Determination of Titration carbonate (VINDTA 3C, Germany). TA of brine was determined by potentiometric titration of 40 mL sample in open cell with 0.05 N hydrochloric acid using a Titrino system (Metrohm, Switzerland). The average standard deviation for DIC and TA, determined from replicate sample analyses from one sample, was within ±2 µmol $kg^{-1}$ for both DIC and TA. Accuracy of the DIC and TA measurements were ±2 µmol $kg^{-1}$ for both DIC and TA estimated using Certified Reference Materials (CRM, provided by A. G. Dickson, Scripps Institution of Oceanography, USA). The $pCO_2$ of brine ($pCO_{2\,b}$) was derived from in situ temperature, salinity, DIC and TA of brine using the carbonate speciation program CO2SYS (Pierrot et al., 2006). We used the carbonate dissociation constants ($K_1$ and $K_2$) of Mehrbach et al. (1973) as refit by Dickson and Millero (1987), and the $KSO_4$ determined by Dickson (1990). The conditional stability constants used to derived $pCO_2$ are strictly only valid for temperatures above 0 °C and salinities between 5 and 50. Studies in spring ice indicated that seawater thermodynamic relationships may be acceptable in warm and low-salinity sea ice (Delille et al., 2007). In sea ice brines at even moderate brine salinities of 80, Brown et al. (2014) found that measured and calculated values of the $CO_2$ system parameters can differ by as much as 40%. On the other hand, because the $CO_2$ system parameters are much more variable in sea ice than in seawater, sea ice measurements demand less precision than those in seawater. Fransson et al. (2015) performed one of few detailed analyses of the internal consistency using four sets of dissociation constants and found that the deviation between measured and calculated DIC varied between ±6 and ±11 µmol $kg^{-1}$, respectively. This error in calculated DIC was considered insignificant in relation to the natural variability in sea ice.

The water equivalent was computed for snow by multiplying snow thickness by snow density (Jonas et al., 2009). Brine volume of sea ice was calculated from the temperature and salinity of sea ice according to Cox and Weeks (1983).

## 3 Results

Biogeosciences Discuss., https://doi.org/10.5194/bg-2017-521
Manuscript under review for journal Biogeosciences
Discussion started: 8 January 2018




### 3.1 Air temperature

Air temperature is shown in Figure 3. During the study period, air temperature varied significantly from a low of –41.3°C (30 January) to a high of +1.7°C (15 June) (Hudson et al., 2015). Even in wintertime (from January to March), rapid increases of air temperature from below –30°C up to –0.2°C (e.g., 18 February), were observed. In springtime (from April to June), the air temperature increased continuously, and from 1 June, air temperatures were near-constant 0°C, although rapid increases (and subsequent decreases) of air temperature to near 0°C were observed on two occasions in mid-May (Cohen et al., 2017).

### 3.2 Characteristics of snow, sea ice, and frost flower

The snow and ice thickness at the observation sites ranged between 0.0 and 60.0 cm and between 15.0 and >200 cm, respectively (Table 1). The thin snow and ice represent newly formed ice in leads. The thickness of the frost flowers ranged from 1.0 to 2.5 cm.

Figure 4 shows vertical profiles of snow and ice temperature and salinity in the top 20 cm of ice. Temperatures within the snowpack depended on the air temperature at the time of observation. However, the bottom of the snow and the surface of the sea ice were relatively warm (T>–7.5°C), except for the frost flower station YI1 and the multi-year ice station OI1 (Figure 4a and Table 2). High salinities (S>18.6) characterized the bottom of the snow and the surface of the sea ice, except for the multi-year ice station OI1 (Figure 4b). At the multi-year ice station OI1, salinity was zero through the snow and top of sea ice. Salinity of frost flowers was up to 92.8 for the thin ice station YI1 (Figure 4b). Snow density and water equivalent ranged from 268 to 400 kg $m^{-3}$ and 11 to 180 kg $m^{-2}$, respectively.

### 3.3 Physical and chemical properties of brine

Biogeosciences Discuss., https://doi.org/10.5194/bg-2017-521
Manuscript under review for journal Biogeosciences
Discussion started: 8 January 2018


292 The brine volume fraction, temperature, salinity, DIC, TA, and calculated $pCO_2$ are
293 summarized in Table 2. Brine volume fraction in top 20 cm of ice was from 9 to 17%,
294 except for the value of 0% at the multi-year ice station OI1 (Table 2). Brine
295 temperatures and salinity ranged from −5.3 to −3.3°C and 51.8 to 86.6, respectively.
296 DIC and TA of brine ranged from 3261 to 4841 μmol $kg^{-1}$ and 3518 to 5539 μmol $kg^{-1}$,
297 respectively. The $pCO_2$ of brine ($pCO_{2\,b}$) (334−693 μatm) was generally higher than
298 that of atmosphere ($pCO_{2\,a}$) (401 ± 7 μatm), except for station FI4.
299
300
301 **3.4 $CO_2$ flux**
302
303 Table 3 summarizes the $CO_2$ flux measurements for each surface condition. For
304 undisturbed natural surface conditions, i.e. measurements directly on the snow surface
305 ($F_{snow}$) or the frost flowers ($F_{ff}$) on young ice, the mean $CO_2$ flux was +0.2 ± 0.2 mmol
306 C $m^{-2}$ $day^{-1}$ for $F_{snow}$ and +1.0 ± 0.6 mmol C $m^{-2}$ $day^{-1}$ for $F_{ff}$. The potential flux in
307 cases when snow or frost flowers had been removed ($F_{ice}$) was +2.5 ± 4.3 mmol C $m^{-2}$
308 $day^{-1}$. The air–sea ice $CO_2$ fluxes measured over the ice surface ($F_{ice}$) increased with
309 increasing difference in $pCO_2$ between brine and atmosphere ($\Delta pCO_{2\,b-a}$) with
310 significant correlation ($R^2 = 0.9$, $p < 0.02$), but this was not the case for $F_{snow}$ ($R^2 = 0.0$,
311 $p < 0.96$).
312
313
314
315 **4 Discussion**
316
317 **4.1 Effect of snow cover on the physical properties of sea ice surface**
318
319 In this study, we examined $CO_2$ fluxes between sea ice and atmosphere in a variety of
320 air temperature conditions from –32 to –3°C and diverse snow and ice conditions (Table
321 2). The bottom of the snow pack and the surface of the sea ice remained relatively warm
322 (>–7.5°C) (Figure 4a, Table 2) except for station OI1, even though air temperature was
323 sometimes below –40°C (Figure 3). Relatively warm ice temperatures were likely due

to the upward heat transport from the bottom of the ice and in cases the thick insulating snow cover (Table 2). Therefore, snow acted as thermal insulator over sea ice, and in general the snow depths observed during N-ICE2015 pointed towards this being representative for first-year and second-year or older ice in the study region in winter 2015 (Rösel et al., 2016a). The young and first-year ice surfaces were characterized by high salinities (Figure 4b). During sea ice formation, upward brine transport to the snow pack occurs (e.g., Toyota et al., 2011). In addition, brine within the sea ice was not completely drained as compared to that of multi-year ice. Furthermore, formation of frost flowers and subsequent wicking up of surface brine into the frost flowers also provides high salinity at the surface of sea ice (Kaleschke et al., 2004; Geilfus et al., 2013; Barber et al., 2014; Fransson et al., 2015) as observed in this study (S>92) (Figure 4b). Snowfall over the frost flowers would have preserved the high salinity at the bottom of snow pack and top of sea ice for young and first-year ice.

As a result of the combination of the relatively high temperature and high salinity at the top of sea ice, brine volume fractions in the upper parts of the sea ice were high, up to 17% (Table 2). It has been shown that ice permeability increases by an order of magnitude when brine volume fraction > 5%, which would correspond to a temperature of –5°C for a bulk ice salinity of 5 – the so called "law of fives" (Golden et al., 1998; Pringle et al., 2009; Zhou et al., 2013). Because sea ice temperatures was low and thereby reduced permeability in winter season, generally, air–sea ice $CO_2$ flux is at its minimum in the winter (e.g., Delille et al., 2014). However, in our study, the brine volume fractions were generally >9%, except for station OI1 with fresh ice at the surface, providing conditions for active gas exchange within sea ice and between sea ice and atmosphere. This situation was likely made possible due to the thick snow cover and relatively thin and young sea ice.

### 4.2 $CO_2$ fluxes over different sea-ice surface types

The $CO_2$ flux measurements over different surface conditions indicate that the snow on sea ice affect the magnitude of air–sea ice $CO_2$ flux (Table 3). For undisturbed natural

Biogeosciences Discuss., https://doi.org/10.5194/bg-2017-521
Manuscript under review for journal Biogeosciences
Discussion started: 8 January 2018


surface conditions, the mean $CO_2$ flux measured directly over snow-covered first-year ice and young ice with frost flowers ($F_{snow}$ and $F_{ff}$) was lower than the potential flux obtained directly over the ice surface after removing snow ($F_{ice}$).

$F_{ff}$ indicates that the frost flower surface on young thin ice is a $CO_2$ source to the atmosphere. Frost flowers are known to promote gas flux, such as $CO_2$, from the sea ice to the atmosphere (Geilfus et al., 2013; Barber et al., 2014; Fransson et al., 2015). At multi-year ice station OI1, neither snow or ice surface acted as a $CO_2$ source/sink. The surface of multi-year ice did not contain any brine (Figure 4 and Table 2), and the top of the ice was clear, colorless and very hard, suggesting superimposed formation at the top of sea ice. This situation would be similar as for freshwater-ice and superimposed-ice as these non-porous media block gas exchange effectively at the sea ice surface (Delille et al., 2014). Snow-ice and superimposed-ice were frequently found in second-year ice cores during N-ICE2015 (Granskog et al., 2017), so the 'blocking' of gas exchange in second-year and multi-year ice may be a widespread process in the Arctic.

The magnitude of $F_{snow}$ is less than $F_{ice}$ (Table 3) indicating that the potential $CO_2$ flux through sea ice decreased due to the presence of snow. Previous studies have shown that snow accumulation over sea ice effectively impede $CO_2$ exchange (Nomura et al., 2013; Brown et al., 2015). Nomura et al. (2013) reported that water equivalent of the snow is an important factor that controls the $CO_2$ exchange through a snowpack. Comparisons between stations FI5 and FI6 for $F_{snow}/F_{ice}$ ratio (0.2 for FI5 and 0.0 for FI6) and water equivalent (11 kg $m^{-2}$ for FI5 and 127 kg $m^{-2}$ for FI6) indicate that the $CO_2$ flux is affected by snow properties (density and depth). Although the potential $CO_2$ flux through the sea ice surface decreased by the presence of snow (Table 3), the snow surface still presents a $CO_2$ source to the atmosphere for low snow density and shallow depth conditions (e.g., +0.6 mmol C $m^{-2}$ $day^{-1}$ for FI5).

### 4.3 Comparison to earlier studies on sea-ice to air $CO_2$ flux



387 The $CO_2$ fluxes measured over the undisturbed natural surface conditions ($F_{snow}$ and $F_{ff}$)
388 in this study ranged from +0.1 to +1.6 mmol C $m^{-2}$ $day^{-1}$ (Table 3), which are at the
389 lower end of the reported range based on the chamber method and eddy covariance
390 method for natural and artificial sea ice (–259.2 to +74.3 mmol C $m^{-2}$ $day^{-1}$)
391 (Zemmelink et al., 2006; Nomura et al., 2006, 2010a, 2010b, 2013; Miller et al., 2011;
392 Papakyriakou and Miller, 2011; Geilfus et al., 2012, 2013; 2014; Barber et al., 2014;
393 Delille et al., 2014; Sørensen et al., 2014; Brown et al., 2015; Kotovitch et al., 2016).
394 Direct comparison to previous studies is complicated because $CO_2$ flux measurements
395 with both chamber and eddy covariance techniques were used during different condition
396 for season and ice surface characteristics. The footprint size of $CO_2$ exchange measured
397 with the two approaches (Zemmelink et al., 2006, 2008; Burba et al., 2008; Amiro,
398 2010; Miller et al., 2011; Papakyriakou and Miller, 2011; Sørensen et al., 2014; Miller
399 et al., 2015) may be one reason for the large difference.
400
401 When we compare our natural $CO_2$ flux range (+0.1 to +1.6 mmol C $m^{-2}$ $day^{-1}$ for $F_{snow}$
402 and $F_{ff}$) (Table 3) to estimates made by the chamber method in previous studies (–5.2 to
403 +6.7 mmol C $m^{-2}$ $day^{-1}$) (Nomura et al., 2006, 2010a, 2010b, 2013; Geilfus et al., 2012,
404 2013; 2014; Barber et al., 2014; Delille et al., 2014; Brown et al., 2015; Kotovitch et al.,
405 2016) (these studies include both natural and potential fluxes), our $CO_2$ fluxes are at the
406 lower end. However, our potential $CO_2$ flux ($F_{ice}$) was a larger $CO_2$ source (+11.8 mmol
407 C $m^{-2}$ $day^{-1}$) than reported in previous studies (+6.7 mmol C $m^{-2}$ $day^{-1}$). In our study,
408 the maximum potential flux (e.g., +11.8 mmol C $m^{-2}$ $day^{-1}$) was obtained for $F_{ice}$ at
409 station FI6 (Table 3). In this situation, $\Delta pCO_{2\,b-a}$ (293 µatm) was the highest (Table 2),
410 and it is reasonable to consider this as the highest magnitude of positive $CO_2$ flux within
411 our study. However, a previous study by closed chamber method showed that even for a
412 similar $\Delta pCO_{2\,b-a}$ (297 µatm) and magnitude for the brine volume fraction (10–15%),
413 the $CO_2$ flux was +0.7 mmol C $m^{-2}$ $day^{-1}$ for artificial sea ice with no snow in the tank
414 experiment (Nomura et al., 2006). In the following, we will discuss this difference.
415
416 The $CO_2$ flux (F) between the sea ice and overlying air can be expressed by the
417 following equation,
418

$$F = r_b\ k\ \alpha\ \Delta pCO_{2\ b-a},$$

where $r_b$ is the ratio of surface of the brine channel to sea ice surface, and we assume that the value of $r_b$ is equal to brine volume fraction, k is the gas transfer velocity, α is the solubility of $CO_2$ (Weiss, 1974), and $\Delta pCO_{2\ b-a}$ is the difference in $pCO_2$ between brine and atmosphere. The equation is based on the fact that $CO_2$ transfer between seawater and air is controlled by processes in the near-surface water (Liss, 1973). The gas transfer velocity (k) calculated from F, $r_b$, α and $\Delta pCO_{2\ b-a}$ was 5.12 m day$^{-1}$ for $F_{ice}$ at station FI6 and 0.29 m day$^{-1}$ for the tank experiment examined in Nomura et al. (2006). This result clearly indicates that the gas transfer velocity for $F_{ice}$ at station FI6 is higher than that of tank experiment examined in Nomura et al. (2006) even with very similar $\Delta pCO_{2\ b-a}$ and brine volume fraction.

Here, we surmise that the gas transfer velocity and thereby $CO_2$ flux is greatly enhanced by the temperature difference between sea ice surface and atmosphere. Previous studies indicate that there is an unstable air density gradient in a dry snowpack due to basal heating and the strong temperature difference develops between bottom and top of snow (e.g., Powers et al., 1985; Severinghaus et al., 2010), which enhances the flow of air through the snowpack. We propose that the mixing and transport of gas within the snowpack could also occur over sea ice. Because temperatures at the bottom of snow and the top of sea ice were relatively warm due to a thick insulating snow over sea ice, there was a strong temperature difference between sea ice surface and atmosphere when air temperature was low (Figure 4a and Table 2). For station FI6, temperature difference between sea ice surface and atmosphere was 20.2°C after snow removal. On the other hand, in the tank experiment by Nomura et al. (2006), the temperature difference between sea ice surface (top 1.5 cm) and air in the headspace was only 4.5°C. Figure 5 shows the relationship between mean air–sea ice $CO_2$ fluxes and temperature difference between ice and atmosphere. The strong dependence of $CO_2$ flux with temperature difference ($T_{ice}$–$T_a$) was observed, especially for $F_{ff}$ and $F_{ice}$ ($R^2 > 0.7$, $p < 0.01$) (Figure 5). Due to the high brine volume fractions (Table 2), sea ice surface had enough permeability for gas exchange. In addition, ice temperatures were similar for young and first-year ice (Figure 5, Table 2), indicating that $pCO_2$ at the top of sea ice and $CO_2$ flux

would be of similar order of magnitude if thermodynamic processes dominated. Therefore, our result suggest that the $CO_2$ fluxes even over the frost flower as natural condition, would be enhanced by the upward transport of air containing high $CO_2$ from the surface of sea ice to the atmosphere due to the strong temperature difference between sea ice surface and atmosphere. Although the presence of snow on sea ice has potential to produce a larger temperature difference between sea ice surface and atmosphere and promote the upward transport, the magnitude of the $CO_2$ flux decreased due to the presence of snow. However, for young sea ice likely the frost flower conditions, ice surface temperature was warm (Table 2), suggesting that $CO_2$ flux would be enhanced by the large temperature difference between sea ice surface and atmosphere.

## 5 Conclusions

We measured $CO_2$ fluxes along with sea ice and snow physical and chemical properties over first-year and young sea ice north of Svalbard in the Arctic ice pack. Our results suggest that young thin snow-free ice, with or without frost flowers, is a source of atmospheric $CO_2$ due to the high $pCO_2$ and salinity and relatively high sea ice temperature. Although the potential $CO_2$ flux through the sea-ice surface decreased due to the presence of snow, snow surface still presents a modest $CO_2$ source to the atmosphere for low snow density and shallow depth situations. The highest ice to air fluxes were observed over thin young sea ice formed in leads. During N-ICE2015 the ice pack was dynamic, and formation of open water was associated with storms, where new ice was formed. Open leads and storm periods were important for air-to-sea $CO_2$ fluxes (Fransson et al., 2017), due to undersaturation of the surface waters, while the subsequent ice growth in these leads becomes important for the ice-to-air $CO_2$ fluxes in winter due to the fact that the flux from young ice is an order of magnitude larger than from snow-covered first-year ice.

High salinity and high sea ice temperature resulted in high brine volume fractions. Given the fact that Arctic sea ice is shifting from multi-year ice to first-year ice (e.g., Stroeve et al., 2012; Meier et al., 2014), the area of thinner seasonal ice has increased. Therefore, the amount of $CO_2$ released from sea ice surface to the atmosphere will be an important fraction of the total $CO_2$ released by the Arctic Ocean. The dynamics of the thinner ice pack, through formation of leads and new ice, will become an important in the gas fluxes from the ice pack.

## 6 Data availability

Data used in this paper will be available at Norwegian Polar Data Centre (data.npolar.no).

## 7 Acknowledgments

We would like to express heartfelt thanks to the crew of R/V Lance and all members of the N-ICE2015 expedition for their support in conducting the field work. This work was supported by the Japan Society for the Promotion of Science (#15K16135, #24-4175), Research Council of Norway (KLIMAFORSK programme, grant 240639), the Centre of Ice, Climate and Ecosystems (ICE) at the Norwegian Polar Institute through the N-ICE project, the Ministry of Climate and Environment and the Ministry of Foreign Affairs of Norway and the Grant for Joint Research Program of the Institute of Low Temperature Science, Hokkaido University. AF, MC and MAG were supported by the flagship research program "Ocean acidification and ecosystem effects in Northern waters" within the FRAM-High North Research Centre for Climate and the Environment.



514

515 **Reference list**

516

517 Amiro, B.: Estimating annual carbon dioxide eddy fluxes using open-path analysers for
518 cold forest sites. Agr. Forest Meteorol., 150, 15, 1366–1372. 2010.

519

520 Barber, D. G., Ehn, J. K., Pućko, M., Rysgaard, S., Deming, J. W. and co-authors: Frost
521 flowers on young Arctic sea ice: The climatic, chemical and microbial significance of
522 an emerging ice type. J Geophys. Res.-Atmos. doi: 10.1002/2014JD021736. 2014.

523

524 Brown, K. A, Miller, L. A., Davelaar, M., Francois, R., and Tortell P. D.: Over-
525 determination of the carbonate system in natural sea ice brine and assessment of
526 carbonic acid dissociation constants under low temperature, high salinity conditions.
527 Mar. Chem 165: 36–45. doi: 10.1016/j.marchem.2014.07.005. 2014.

528

529 Brown, K. A., Miller, L.A., Mundy, C. J., Papakyriakou, T., Francois, R., and co-
530 authors: Inorganic carbon system dynamics in landfast Arctic sea ice during the early-
531 melt period. J. Geophys. Res. Oceans, 120, 3542–3566.
532 http://dx.doi.org/10.1002/2014JC010620. 2015.

533

534 Burba, G., McDermitt, D., Grelle, A., Anderson, D., and Xu, L.: Addressing the
535 influence of instrument surface heat exchange on the measurements of $CO_2$ flux from
536 open-path gas analyzers, Global Change Biol., 14, 8, 1854–1876, 2008.

537

538 Cohen, L., Hudson, S. R., Walden, V. P., Graham, R. M., and Granskog, M. A.:
539 Meteorological conditions in a thinner Arctic sea ice regime from winter through
540 summer during the Norwegian young sea ICE expedition (N-ICE2015), J. Geophys. Res.
541 Atmos., 122, 7235–7259, doi:10.1002/2016JD026034, 2017.

542

543 Cox, G. F. N., and Weeks W. F.: Equations for determining the gas and brine volumes
544 in sea-ice samples, J. Glaciol., 29, 306–316, 1983.

545

546 Delille, B., Jourdain, B., Borges, A. V., Tison, J.-L., and Delille, D.: Biogas ($CO_2$, $O_2$,
547 dimethylsulfide) dynamics in spring Antarctic fast ice, Limnol. Oceanogr., 52, 1367–
548 1379, 2007.
549
550 Delille, B., Vancoppenolle, M., Geilfus, N.-X.. Tilbrook, B. Lannuzel.D., and co-
551 authors: Southern Ocean $CO_2$ sink: the contribution of the sea ice, J. Geophys. Res.
552 Oceans. 119 (9), 6340–6355, 2014.
553
554 Dickson, A. G., and Millero F. J.: A comparison of the equilibrium constants for the
555 dissociation of carbonic acid in seawater media, Deep-Sea Res. 34, 1733–1743, 1987.
556
557 Dickson, A. G.: Thermodynamics of the dissociation of boric acid in synthetic seawater
558 from 273.15 to 318.15 K, Deep-Sea Res. 37, 755–766, 1990.
559
560 Dickson, A. G., Sabine, C. L., and Christian, J. R. Eds.: Guide to Best Practices for
561 Ocean $CO_2$ Measurements, PICES Special Publication, 3, 191 pp, 2007.
562
563 Fransson, A., Chierici, M., Miller, L. A., Carnat, G., Thomas, H., and co-authors:
564 Impact of sea ice processes on the carbonate system and ocean acidification state at the
565 ice-water interface of the Amundsen Gulf, Arctic Ocean, J. Geophys. Res., 118, 1–23,
566 doi:10.1002/2013JC009164, 2013.
567
568 Fransson, A., Chierici, M., Abrahamsson, K., Andersson, M., Granfors, A., and co-
569 authors: $CO_2$-system development in young sea ice and $CO_2$ gas exchange at the ice/air
570 interface mediated by brine and frost flowers in Kongsfjorden, Spitsbergen, Ann.
571 Glaciol., 56, 69, doi: 10.3189/2015A0G69A563, 2015.
572
573 Fransson, A., Chierici, M., Skjelvan, I., Olsen, A., Assmy, P., Peterson, A. K., Ward,
574 B.: Effects of sea-ice and biogeochemical processes and storms on under-ice water f
575 $CO_2$ during the winter-spring transition in the high Arctic Ocean: Implications for sea-
576 air $CO_2$ fluxes, J. Geophys. Res. Oceans, 122(7), 5566–5587.
577 https://doi.org/10.1002/2016JC012478. 2017.

578

579 Geilfus, N.-X., Carnat, G., Papakyriakou, T., Tison, J.-L., Else, B. and co-authors:
580 Dynamics of $pCO_2$ and related air–ice $CO_2$ fluxes in the Arctic coastal zone (Amundsen
581 Gulf, Beaufort Sea), J. Geophys. Res., 117, C00G10, doi:10.1029/2011JC007118, 2012.
582
583 Geilfus, N.-X., Carnat, G., Dieckmann, G. S., Halden, N., Nehrke, G., and co-authors:.
584 First estimates of the contribution of $CaCO_3$ precipitation to the release of $CO_2$ to the
585 atmosphere during young sea ice growth, J. Geophys. Res., 118:244–255.
586 http://dx.doi.org/10.1029/2012JC007980, 2013.
587
588 Geilfus, N.-X., Tison, J.-L., Ackley, S. F., Galley, R. J., Rysgaard, S., and co-authors:
589 Sea ice $pCO_2$ dynamics and air–ice $CO_2$ fluxes during the Sea Ice Mass Balance in the
590 Antarc-tic (SIMBA) experiment – Bellingshausen Sea, Antarctica, The Cryosphere, 8,
591 2395–2407, doi:10.5194/tc-8-2395-2014, 2014.
592
593 Geilfus, N.-X., Galley, R. J., Crabeck, O., Papakyriakou, T., Landy, J., Tison, J.-L. and
594 Rysgaard, S.:I norganic carbon dynamics of melt-pond-covered first-year sea ice in the
595 Canadian Arctic, Biogeosci., 12, 2047–2061, www.biogeosciences.net/12/2047/2015/,
596 doi:10.5194/bg-12-2047-2015, 2015.
597
598 Gleitz, M., Vonderlo, M. R., Tomas, D. N., Dieckmann, G. S. and Millero F. J.:
599 Comparison of summer and winter inorganic carbon, oxygen and nutrient
600 concentrations in Antarctic sea ice brine, Mar. Chem., 51, 81–89, 1995.
601
602 Golden, K. M., Ackley, S. F. and Lytle, V. I.: The percolation phase transition in sea ice,
603 Science, 282, 2238–2241, 1998.
604
605 Granskog, M. A., Assmy, P., Gerland, S., Spreen, G., Steen, H., and co-authors: Arctic
606 research on thin ice: Consequences of Arctic sea ice loss, Eos Transactions AGU, 97,
607 22–26, doi:10.1029/2016EO044097, 2016.
608

609 Granskog, M. A., Rösel, A., Dodd, P. A., Divine, D., Gerland, S., and co-authors: Snow
610 contribution to first-year and second-year Arctic sea ice mass balance north of Svalbard,
611 J. Geophys. Res. Oceans, 122, 2539-2549, doi: 10.1002/2016JC012398, 2017.
612
613 Hudson, S. R., Cohen, L., and Walden, V.: N-ICE2015 surface meteorology (Data set),
614 Norwegian Polar Institute, doi: 10.21334/npolar.2015.056a61d1, 2015.
615
616 Inoue, H. Y. and Ishii M.: Variations and trends of $CO_2$ in the surface seawater in the
617 Southern Ocean south of Australia between 1969 and 2002, Tellus, Ser. B, 57, 58–69,
618 2005.
619
620 Jonas, T., Marty, C., and Magnusson, J.: Estimating the snow water equivalent from
621 snow depth measurements in the Swiss Alps, J. Hydrol., 378, 161–167, 2009.
622
623 Kaleschke, L., Richter, A., Burrows, J., Afe, O., Heygster, G., and co-authors: Frost
624 flowers on sea ice as a source of sea salt and their influence on tropospheric halogen
625 chemistry, Geophys. Res. Lett., 31, L16114, doi:10.1029/2004GL020655, 2004.
626
627 Kotovitch, M., Moreau, S., Zhou, J., Vancoppenolle, M., Dieckmann, G. S., and co-
628 authors: Air–ice carbon pathways inferred from a sea ice tank experiment, Elementa:
629 Science of the Anthropocene, 4, 1, doi10.12952/journal.elementa.000112, 2016.
630
631 Lindsay, R., and Schweiger, A.: Arctic sea ice thickness loss determined using
632 subsurface, aircraft, and satellite observations, The Cryosphere, 9(1), 269–283,
633 doi:10.5194/tc-9-269-2015, 2015.
634
635 Liss, P. S.: Processes of gas exchange across an air-water interface, Deep-Sea Res. 20,
636 221–238, 1973.
637
638 Massom, R.A., Eicken, H., Haas, C., Jeffries, M. O., Drinkwater, M. R., and other co-
639 authors: Snow on Antarctic sea ice, Reviews of Geophysics, 39, 413–445, 2001.
640

641 Mehrbach, C., Culberson, C. H., Hawley, J. E., and Pytkowicz P. M.: Measurement of
642 the apparent dissociation constant of carbonic acid in seawater at atmospheric pressure,
643 Limnol. Oceanogr., 18, 897–907, 1973.
644
645 Meier, W. N., Hovelsrud, G. K., van Oort, B. E. H., Key, J. R., Kovacs, K. M., and co-
646 authors: Arctic sea ice in transformation: A review of recent observed changes and
647 impacts on biology and human activity, Rev. Geophys., 52, 185–217,
648 doi:10.1002/2013RG000431, 2014.
649
650 Miller, L. A., Papakyriakou, T. N., Collins, R. E., Deming, J. W., Ehn, J. K., and co-
651 authors: Carbon dynamics in sea ice: A winter flux time series, J. Geophys. Res., 116,
652 C02028, doi:10.1029/2009JC006058, 2011.
653
654 Miller, L. A., Fripiat, F., Else, B. G. T., Bowman, J. S., Brown, K. A., and co-authors:.
655 Methods for Biogeochemical Studies of Sea Ice: The State of the Art, Caveats, and
656 Recommendation, Elementa, 3, 000038, doi:10.12952/journal.elementa.000038, 2015.
657
658 Nomura, D., Inoue, H. Y., and Toyota, T.: The effect of sea-ice growth on air–sea $CO_2$
659 flux in a tank experiment, Tellus, Ser. B, 58, 418–426, 2006.
660
661 Nomura, D., Inoue, H. Y., Toyota, T., and Shirasawa, K.: Effects of snow, snowmelting
662 and refreezing processes on air–sea-ice $CO_2$ flux, J. Glaciol., 56, 196, 262–270, 2010a.
663
664 Nomura, D., Eicken, H., Gradinger, R., and Shirasawa, K.: Rapid physically driven
665 inversion of the air-sea ice $CO_2$ flux in the seasonal landfast ice off Barrow, Alaska
666 after onset of surface melt, Cont. Shelf Res., 30, 1998–2004, 2010b.
667
668 Nomura, D., Granskog, M. A., Assmy, P., Simizu, D., and Hashida, G.: Arctic and
669 Antarctic sea ice acts as a sink for atmospheric $CO_2$ during periods of snow melt and
670 surface flooding, J. Geophys. Res. Oceans, 118, 6511–6524, 2013.
671

672 Merkouriadi, I., Gallet, J.-C., Graham, R. M., Liston, G. E., Polashenski, C., Rösel, A.,
673 and Gerland, S.: Winter snow conditions on Arctic sea ice north of Svalbard during the
674 Norwegian young sea ICE (N-ICE2015) expedition, J. Geophys. Res. Atmos., 122,
675 doi:10.1002/2017JD026753, 2017.
676
677 Papadimitriou, S., Kennedy, H., Norman, L., Kennedy, D. P., Dieckmann, G. S., and
678 co-authors: The effect of biological activity, $CaCO_3$ mineral dynamics, and $CO_2$
679 degassing in the inorganic carbon cycle in sea ice in late winter-early spring in the
680 Weddell Sea, Antarctica, J. Geophys. Res. 117, C08011, doi:10.1029/2012JC008058,
681 2012.
682
683 Papakyriakou, T., and Miller, L. A.: Springtime $CO_2$ exchange over seasonal sea ice in
684 the Canadian Arctic Archipelago, Ann. Glaciol., 52, 57, 215–224, 2011.
685
686 Parmentier, F. J. W., Christensen, T. R., Sørensen, L. L., Rysgaard, S., McGuire, A. D.,
687 and co-authors: The impact of lower sea-ice extent on Arctic greenhouse-gas exchange,
688 Nature Climate Change, 3, 195–202, doi:10.1038/nclimate1784, 2013.
689
690 Pierrot, D., Lewis, E. and Wallace, D. W. R.: MS Excel Program Developed for $CO_2$
691 System Calculations, ORNL/CDIAC-105a. Carbon Dioxide Information Analysis
692 Center, Oak Ridge National Laboratory, U.S. Department of Energy, Oak Ridge,
693 Tennessee, doi: 10.3334/CDIAC/otg.CO2SYS_XLS_CDIAC105a, 2006.
694
695 Powers, D., Oneill, K., and Colbeck, S. C.: Theory of natural convection in snow, J.
696 Geophys. Res.-Atmos., 90, 10641–10649, doi:10.1029/Jd090id06p10641, 1985.
697
698 Pringle, D. J., Miner, J. E., Eicken, H., and Golden, K. M.: Pore space percolation in sea
699 ice single crystals, J. Geophys. Res., 114, C12017, doi:10.1029/2008JC005145, 2009.
700
701 Rysgaard, S., Søgaard, D. H., Cooper, M., Pucko, M., Lennert, K., and co-authors:
702 Ikaite crystal distribution in winter sea ice and implications for $CO_2$ system dynamics,
703 The Cryosphere, 7, 707–718, doi:10.5194/tc-7-707-2013, 2013.

Rösel, A., Polashenski, C. M., Liston, G. E., King, J. A., Nicolaus, M. and co-authors: N-ICE2015 snow depth data with Magna Probe (Data set), Norwegian Polar Institute, doi:10.21334/npolar.2016.3d72756d, 2016a.

Rösel, A., Divine, D., King, J. A., Nicolaus, M., Spreen, G., and co-authors: N-ICE2015 total (snow and ice) thickness data from EM31 (Data set), Norwegian Polar Institute, doi:10.21334/npolar.2016.70352512, 2016b.

Schindlbacher, A., Zechmeister-Boltenstern, S., Glatzel, G., and Jandl R.: Winter soil respiration from an Austrian mountain forest, Agric, For. Meteorol., 146, 205–215, doi:10.1016/j.agrformet.2007.06.001, 2007.

Severinghaus, J. P., Albert, M. R., Courville, Z. R., Fahnestock, M. A., Kawamura, K., and co-authors: Deep air convection in the firn at a zero-accumulation site, central Antarctica, Earth Planet. Sci. Lett., 293, 359–367, doi:10.1016/J.Epsl.2010.03.003, 2010.

Stroeve, J. C., Serreze, M. C., Holland, M. M., Kay, J. E., Maslanik, J., and Barrett, A. P.: The Arctic's rapidly shrinking sea ice cover: a research synthesis, Climatic Change, 110, 1005, doi:10.1007/s10584-011-0101-1, 2012.

Sørensen, L. L, Jensen, B., Glud, R. N., McGinnis, D. F., and Sejr, M. K.: Parameterization of atmosphere-surface exchange of $CO_2$ over sea ice, The Cryosphere, 8: 853–866. doi:10.5194/tc-8-853-2014, 2014.

Takagi, K., Nomura, M., Ashiya, D., Takahashi, H., Sasa, K., and co-authors: Dynamic carbon dioxide exchange through snowpack by wind-driven mass transfer in a conifer-broadleaf mixed forest in northernmost Japan, Global Biogeochem. Cycles, 19, GB2012, doi:10.1029/2004GB002272, 2005.

735 Toyota, T., Massom, R., Tateyama, K., Tamura, T., and Fraser, A.: Properties of snow
736 overlying the sea ice off East Antarctica in late winter 2007, Deep Sea Res. II, 58,
737 1137–1148, 2011.
738
739 Vancoppenolle, M., Meiners, K. M., Michel, C., Bopp, L., Brabant, F., and co-authors:
740 Role of sea ice in global biogeochemical cycles: emerging views and challenges, Quat.
741 Sci. Rev., 79, 207–230, 2013.
742
743 Weiss, R. F.: Carbon dioxide in water and seawater: the solubility of a non-ideal gas,
744 Mar. Chem., 2, 203–215, 1974.
745
746 Zemmelink, H. J., Delille, B., Tison, J.-L., Hintsa, E. J., Houghton, L., and co-authors:.
747 $CO_2$ deposition over the multi-year ice of the western Weddell Sea, Geophys. Res. Lett.,
748 33, L13606, doi:10.1029/2006GL026320, 2006.
749
750 Zemmelink, H. J., Dacey, J. W. H., Houghton, L., Hintsa. E. J., and Liss, P. S.:
751 Dimethylsulfide emissions over the multi-year ice of the western Weddell Sea, Geophys.
752 Res. Lett., 35, L06603, doi:10.1029/2007GL031847, 2008.
753
754 Zhou, J., Delille**,** B., Eicken, H., Vancoppenolle, M., Brabant, F., and co-authors:
755 Physical and biogeochemical properties in landfast sea ice (Barrow, Alaska): Insights
756 on brine and gas dynamics across seasons, J. Geophys. Res. 118, 6, 3172–3189, 2013.
757
758
759
760 **Figure captions**
761
762 Figure 1. Location map of the sampling area north of Svalbard during N-ICE2015.
763 Image of the sea ice concentrations (a) and station map (b) were derived from Special
764 Sensor Microwave Imager (SSM/I) satellite data for mean of February 2015 and from
765 Sentinel-1 (Synthetic Aperture Radar Sensor) satellite data, respectively.
766

767 Figure 2. Photographs of the $CO_2$ flux chamber system at station YI1 north of Svalbard
768 on Friday 13 March 2015. $CO_2$ flux chamber was installed over the frost flower on the
769 new thin ice in the refreezing lead.
770
771 Figure 3. Time series of air temperature measured at the weather mast over the ice floe
772 (10 m height). Blank period indicates no data. Colored symbols indicate the date for the
773 chamber flux measurements. The horizontal dashed line indicates air temperature = 0°C.
774
775 Figure 4. Vertical profiles of temperature (a) and salinity (b) in snow and sea ice (top 20
776 cm). The horizontal line indicates snow–ice interface. Shaded area indicates sea ice. For
777 stations FI7 and YI2 and 3, we have no salinity data.
778
779 Figure 5. Relationships between mean air–sea ice $CO_2$ fluxes and temperature
780 difference between ice ($T_{ice}$) and atmosphere ($T_a$) (circle) and ice temperature (Tice)
781 (top 20 cm) (cross) for $F_{snow}$ (blue), $F_{ff}$ (green) and $F_{ice}$ (red) for young and first-year sea
782 ice.
783
784
785
786 **Table captions**
787
788 Table 1. Station, date for $CO_2$ flux measurement, position, floe number, surface
789 condition, ice type and thickness of snow, frost flowers, and sea ice.
790
791 a. Sea ice coring and snow sampling was conducted on 5 March 2015.
792
793 b. Sea ice coring and snow sampling was conducted on 10 March 2015.
794
795
796 Table 2. Station, snow density and water equivalent, brine volume fraction, and
797 temperature for sea ice (top 20 cm), brine temperature, salinity, DIC, TA, $pCO_2$ ($pCO_{2\ b}$),
798 and atmospheric temperature, wind speed and $pCO_2$ ($pCO_{2\ a}$)[a].

799

800 a. $pCO_{2\,a}$ (µatm) was calculated from $CO_2$ concentration (ppmv) at Ny-Ålesund,
801 Svalbard (http://www.esrl.noaa.gov/gmd/dv/iadv/) taking into account saturated water
802 vapor and atmospheric pressure during sampling day.
803
804 b. Mean values for snow column.
805
806 c. "−" indicates no data.
807
808
809 Table 3. $CO_2$ flux measured over the snow ($F_{snow}$), frost flower ($F_{ff}$), and ice surface
810 ($F_{ice}$). Values measured directly over undisturbed surfaces (either with frost flowers or
811 on snow surface) at a given station are indicated in bold.
812
813 a. Data of first $CO_2$ flux measurement after removal of snow or frost flower.
814
815 b. "−" means no data.
816
817 c. Data of OI1 was not included.

Biogeosciences Discuss., https://doi.org/10.5194/bg-2017-521
Manuscript under review for journal Biogeosciences
Discussion started: 8 January 2018


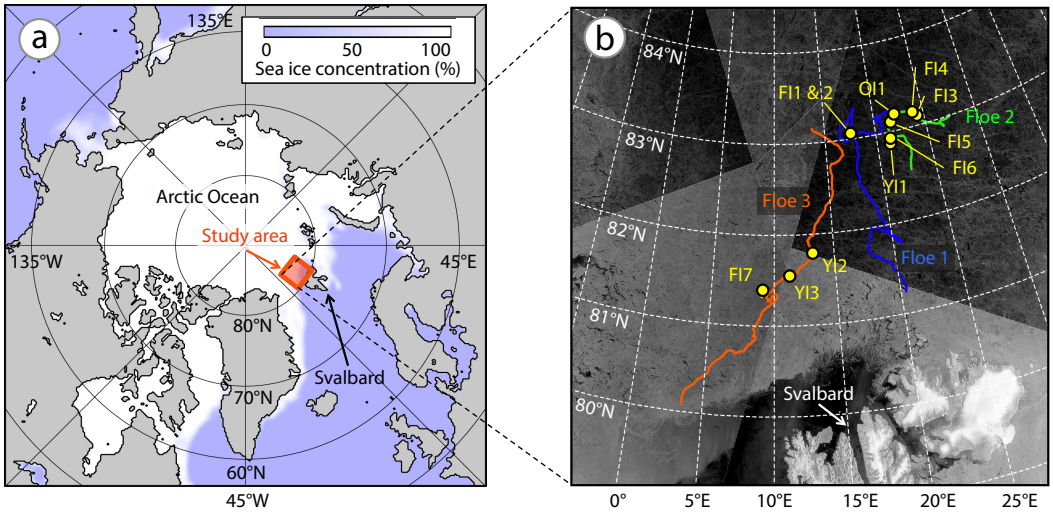


Nomura et al., Figure 1 (Double column size)

Biogeosciences Discuss., https://doi.org/10.5194/bg-2017-521
Manuscript under review for journal Biogeosciences
Discussion started: 8 January 2018


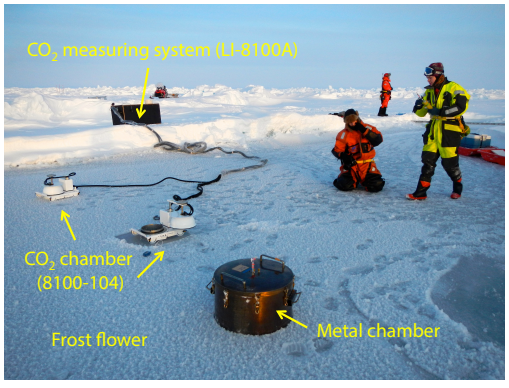


Nomura et al., Figure 2 (Single column size)

Biogeosciences Discuss., https://doi.org/10.5194/bg-2017-521
Manuscript under review for journal Biogeosciences
Discussion started: 8 January 2018


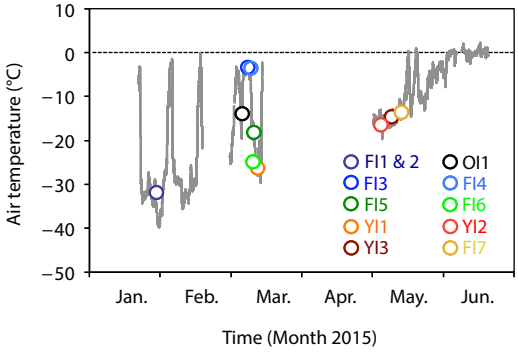


Nomura et al., Figure 3 (Single column size)

Biogeosciences Discuss., https://doi.org/10.5194/bg-2017-521
Manuscript under review for journal Biogeosciences
Discussion started: 8 January 2018


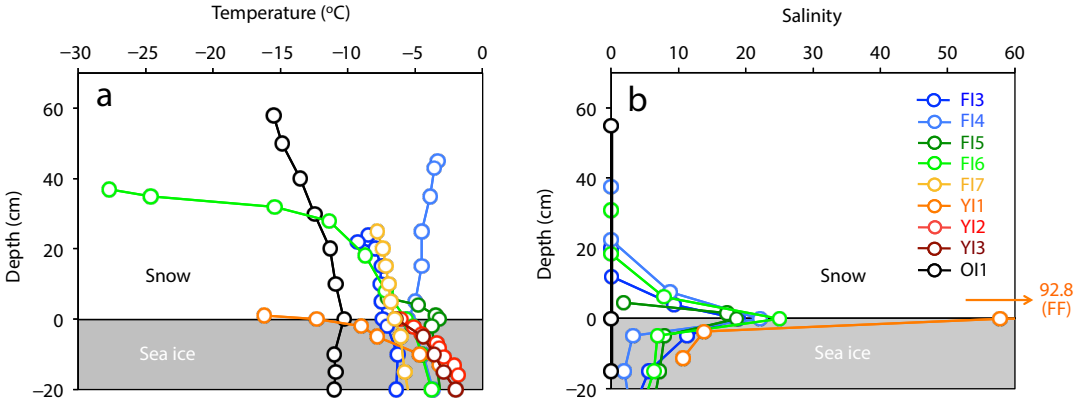


Nomura et al., Figure 4 (Double column size)

Biogeosciences Discuss., https://doi.org/10.5194/bg-2017-521
Manuscript under review for journal Biogeosciences
Discussion started: 8 January 2018


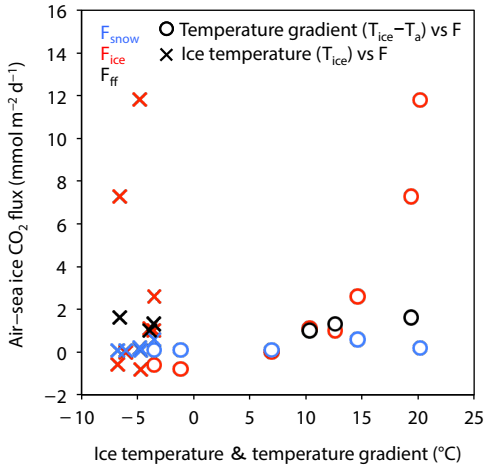


Nomura et al., Figure 5 (Single column size)

Biogeosciences Discuss., https://doi.org/10.5194/bg-2017-521
Manuscript under review for journal Biogeosciences
Discussion started: 8 January 2018


Table 1. Station, position, date for $CO_2$ flux measurement, floe number, surface condition, ice type and thickness of snow, frost flower, and sea ice.

| Station | Position | Date of 2015 | Floe number | Surface condition | Ice type[c] | Thickness (cm) | | |
|---|---|---|---|---|---|---|---|---|
| | | | | | | Snow | Frost flower | Sea ice |
| FI1 | 83°03.77N, 17°34.94E | 28 January | 1 | Frost flower | First-year ice | 0.0 | 1.0 | 37.0 |
| FI2 | 83°03.77N, 17°34.94E | 28 January | 1 | Snow | First-year ice | 8.0 | No | 35.0 |
| FI3 | 83°08.00N, 24°09.02E | 5 and 8 March[a] | 2 | Snow | First-year ice | 29.0 | No | 98.0 |
| FI4 | 83°10.56N, 22°09.42E | 9 March | 2 | Snow | First-year ice | 36.0 | No | 92.0 |
| FI5 | 83°06.02N, 21°38.29E | 10 and 11 March[b] | 2 | Snow | First-year ice | 3.0 | No | 48.0 |
| FI6 | 82°55.36N, 21°25.92E | 12 March | 2 | Snow | First-year ice | 37.0 | No | 69.0 |
| FI7 | 81°22.18N, 08°59.93E | 13 May | 3 | Snow | First-year ice | 26.5 | No | 127.0 |
| YI1 | 82°52.52N, 21°16.54E | 13 March | 2 | Frost flower | Young ice | 0.0 | 1.0 | 15.0 |
| YI2 | 81°46.53N, 13°16.00E | 5 May | 3 | Snow and frost flower mixed | Young ice | 2.5 | 2.5 | 17.5 |
| YI3 | 81°32.45N, 11°17.20E | 9 May | 3 | Snow and frost flower mixed | Young ice | 2.0 | 2.0 | 22.0 |
| OI1 | 83°07.18N, 24°25.59E | 6 March | 2 | Snow | Old ice (multi-year ice) | 60.0 | No | >200 |

a. Sea ice coring, brine and snow sampling was conducted on 5 March 2015.
b. Sea ice coring, brine and snow sampling was conducted on 10 March 2015.
c. Ice type was categorized based on WMO (1970).

Biogeosciences Discuss., https://doi.org/10.5194/bg-2017-521
Manuscript under review for journal Biogeosciences
Discussion started: 8 January 2018




Biogeosciences
Discussions
Open Access
EGU

Table 2. Station, snow density and water equivalent, brine volume fraction and temperature for sea ice (top 20 cm), brine temperature, salinity, DIC, TA, $pCO_2$ ($pCO_{2\,b}$) and atmospheric temperature, wind speed, and $pCO_2$ ($pCO_{2\,a}$)[a].

| Station | Snow | | Sea ice (top 20 cm) | | Brine | | | | | Atmosphere | | |
|---|---|---|---|---|---|---|---|---|---|---|---|---|
| | Density[b] (kg m$^{-3}$) | Water equivalent (kg m$^{-2}$) | Brine volume fraction (%) | Temperature (ºC) | Temperature (ºC) | Salinity | DIC (µmol kg$^{-1}$) | TA (µmol kg$^{-1}$) | $pCO_{2\,b}$ (µatm) | Temperature (ºC) | Wind speed (m second$^{-1}$) | $pCO_{2\,a}$ (µatm) |
| FI1 | –[c] | –[c] | –[c] | –[c] | –[c] | –[c] | –[c] | –[c] | –[c] | −31.6 | 4.0 | 405 |
| FI2 | –[c] | –[c] | –[c] | –[c] | –[c] | –[c] | –[c] | –[c] | –[c] | −31.6 | 4.0 | 405 |
| FI3 | 399 | 104 | 9 | −6.8 | −5.2 | 84.8 | 4628 | 5539 | 427 | −3.3 | 9.0 | 400 |
| FI4 | 400 | 180 | 9 | −4.7 | −5.3 | 86.6 | 4433 | 5490 | 334 | −3.5 | 6.2 | 386 |
| FI5 | 268 | 11 | 17 | −3.5 | −3.3 | 51.8 | 3261 | 3518 | 472 | −18.1 | 6.8 | 389 |
| FI6 | 343 | 127 | 13 | −4.8 | −4.8 | 84.0 | 4841 | 5493 | 693 | −25.0 | 3.6 | 400 |
| FI7 | –[c] | –[c] | –[c] | −6.1 | –[c] | –[c] | –[c] | –[c] | –[c] | −13.0 | 5.8 | 405 |
| Y11 | –[c] | –[c] | 17 | −6.6 | –[c] | –[c] | –[c] | –[c] | –[c] | −26.0 | 2.6 | 402 |
| Y12 | –[c] | –[c] | –[c] | −3.6 | –[c] | –[c] | –[c] | –[c] | –[c] | −16.2 | 4.5 | 407 |
| Y13 | –[c] | –[c] | –[c] | −3.9 | –[c] | –[c] | –[c] | –[c] | –[c] | −14.2 | 6.7 | 410 |
| O11 | –[c] | –[c] | 0 | −10.8 | –[c] | –[c] | –[c] | –[c] | –[c] | −13.5 | 4.7 | 397 |

a. $pCO_{2\,a}$ (µatm) was calculated from $CO_2$ concentration (ppmv) at Ny-Ålesund, Svalbard (http://www.esrl.noaa.gov/gmd/dv/iadv/) taking into account the saturated water vapor and atmospheric pressures at sampling day.
b. Mean values for column.
c. "–" indicates no data.

Biogeosciences Discuss., https://doi.org/10.5194/bg-2017-521
Manuscript under review for journal Biogeosciences
Discussion started: 8 January 2018






Table 3. $CO_2$ flux measured over the snow ($F_{snow}$), frost flower ($F_{ff}$) and ice surface ($F_{ice}$).

| Station | $CO_2$ flux (mmol C $m^{-2}$ $day^{-1}$) (mean ± 1SD) (number of measurement) | | | |
|---|---|---|---|---|
| | Natural flux | | Potential flux | |
| | $F_{snow}$ | $F_{ff}$ | $F_{ice}$ [a] | |
| FI1 | –[a] | **+0.1 ± 0.1** (n=7) | –[b] | |
| FI2 | **+0.4 ± 0.3** (n=13) | –[b] | –[b] | |
| FI3 | **+0.1 ± 0.1** (n=7) | –[b] | −0.6 | |
| FI4 | **+0.1 ± 0.1** (n=6) | –[b] | −0.8 | |
| FI5 | **+0.6 ± 0.3** (n=5) | –[b] | +2.6 | |
| FI6 | **+0.2 ± 0.1** (n=5) | –[b] | +11.8 | |
| FI7 | **+0.1 ± 0.1** (n=10) | –[b] | ±0.0 | |
| YI1 | –[b] | **+1.6 ± 0.2** (n=6) | +7.3 | |
| YI2 | –[b] | **+1.3 ± 0.2** (n=9) | +1.0 | |
| YI3 | –[b] | **+1.0 ± 0.4** (n=8) | +1.1 | |
| OI1 | **+0.1 ± 0.0** (n=6) | –[b] | +0.2 | |
| Mean[c] | **+0.2 ± 0.2** (n=46) | **+1.0 ± 0.6** (n=30) | +2.5 ± 4.3 (n=9) | |

a. Data of first measurement after removal of snow or frost flower.
b. "–" means no data.
c. Data of OI1 was not included.